Available online at www.sciencedirect.com

ScienceDirect

journal homepage: www.elsevier.com/locate/he

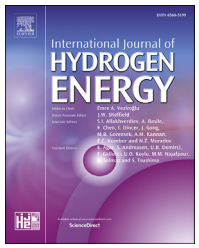

Bio-Energy with Carbon Capture and Storage (BECCS) potential: Production of high purity H_2 from cellulose via Alkaline Thermal Treatment with gas phase reforming of hydrocarbons over various metal catalysts

Maxim R. Stonor [a,c], *Jingguang G. Chen* [a,c,*], *Ah-Hyung Alissa Park* [a,b,c,*]

[a] *Department of Chemical Engineering, Columbia University, New York, NY, USA*
[b] *Department of Earth and Environmental Engineering, Columbia University, New York, NY, USA*
[c] *Lenfest Center for Sustainable Energy, The Earth Institute, Columbia University, New York, NY, USA*

ARTICLE INFO

Article history:
Received 15 February 2017
Received in revised form
7 August 2017
Accepted 10 August 2017
Available online 19 September 2017

Keywords:
Bio-Energy with Carbon Capture and Storage (BECCS)
Hydrogen
Calcium hydroxide
Reforming
Nickel
Catalyst

ABSTRACT

A novel Alkaline Thermal Treatment (ATT) reaction has been proposed as a unique bio-energy with carbon capture & sequestration (BECCS) approach. While our previous study demonstrated that high purity H_2 can be produced from cellulose with a $Ca(OH)_2$ and 10% Ni/ZrO_2 mixture while suppressing CO_2 formation, its complex reaction pathways are not understood. In order to decouple the solid and gas-phase catalytic reactions and improve the overall ATT of biomass, in-situ and ex-situ catalystic ATT reactions have been carried out. A screening of low loading Fe, Cu, Co, Pd, Pt and Ni catalysts showed that Ni was capable of significantly enhancing H_2 production when placed in-situ or ex-situ. This suggested that the ATT of cellulose involves the reforming of intermediates (i.e., gaseous hydrocarbons) to H_2. Catalyst development and reactor design should consider both solid-phase and gas-phase reactions in order to maximize the potential of this BECCS technology.

Introduction

Global energy consumption is expected to increase by 56% by 2040 [1], with the majority of the demand coming from non-OECD countries. Many of these countries use biomass as the primary energy source for cooking and heating, and as their increased use of biomass and fossil fuels is projected, it is important to develop technologies that allow for greener pathways of energy production. The combustion of biomass is often energetically inefficient due to its high moisture content and low energy density [2]. Furthermore, concerns over climate change and anthropogenic CO_2 require energy conversion pathways with a reduced carbon footprint. By integrating a carbon sequestration scheme into

* *Corresponding authors*. Department of Chemical Engineering, Columbia University, New York, NY, USA.
E-mail addresses: jgchen@columbia.edu (J.G. Chen), ap2622@columbia.edu (A.-H.A. Park).
http://dx.doi.org/10.1016/j.ijhydene.2017.08.059
0360-3199/

biomass conversion, the technology could not only be carbon-neutral, but potentially carbon-negative; such technologies are called BECCS (Bio-Energy with Carbon Capture and Storage) [3]. Previous work [4,5] has shown that model biomass compounds (e.g., glucose and cellulose) can be converted to H_2 with suppressed CO_x production via an Alkaline Thermal Treatment (ATT) with NaOH. Our recent study also showed that other hydroxides including $Ca(OH)_2$ can also facilitate the ATT of biomass, particularly in the presence of Ni-based catalysts, although its exact mechanism is still unknown [6].

The role of calcium-based compounds on cellulose conversion reactions is documented to some degree in literature, although not specifically for the ATT process. For instance, CaO has been reported to promote the water-gas shift (WGS) reaction, and hence, H_2 production by acting as a CO_2 sorbent [7–9]. Others also reported that CaO and $Ca(OH)_2$ are effective in improving the yield of H_2 through the cracking of tars and gasification of chars to light gases during biomass conversion [9–12]. Similarly, our previous study on the enhanced WGS reaction in the presence of $Mg(OH)_2$ slurry revealed that in-situ mineralization of CO_2 can significantly improve the H_2 formation from syn-gas [13].

Even the addition of relatively inert materials such as alkali earth metal chlorides (e.g., $CaCl_2$) can also impact the extent of cellulose pyrolysis by increasing the amount of low molecular weight products from the cracking of levoglucosan and 5-HMF [14]. In general, the decomposition of cellulose into lower molecular weight products is the desired route as it is known that small organic compounds such as formic, glycolic and acetic acid can readily be converted to light gases [4,15–17]. Studies have shown that the type of metal cation (e.g., Na, K, Ca) may also play an important role in biomass pyrolysis [18,19].

Furthermore, there are specific studies related to biomass degradation in the presence of alkali. The alkaline degradation of cellulose is a complex multi-step process including end-wise degradation (also known as 'peeling' or 'unzipping'), random alkaline scission as well as oxidative alkaline degradation [20,21]. In the presence of alkali, main degradation products of cellulose via the peeling process is 3-deoxy-2-C-(hydroxymethyl)-*erythro*- and threo-pen-tonic acids (D-glucoisosaccharinic acids) [21]. The addition of calcium ions has shown to enhance such cellulose degradation process by catalysing the conversion of cellulose decomposition intermediates to D-glucoisosaccharinic acids [22]. At temperatures above 443 K, random alkaline scission of the β-1,4-glycosidic linkages also occurs and thus results in further cellulose degradation through the "peeling" of the cellulose fragments [23]. Studies on the alkaline degradation of monosaccharides explain how calcium catalyses benzilic acid rearrangement to promote the production of glucoisosaccharinic acids, whereas NaOH degrades monosaccharides via the fragmentation to glycolic and formic acids [24,25]. While the ATT of cellulose is not identical to the aforementioned reactions and processes it provides an understanding of how the fragmentation of cellulose occurs under alkaline conditions and foundation for the discussion in this study.

In addition to the presence of hydroxide, catalysts also play an important role in the ATT of cellulose. Nickel is one of the most popular catalytic metals due to its low cost, proven catalytic reforming ability, and ability to promote H_2 yield from various feed-stocks in a multitude of reaction conditions [26–33]. Studies have shown that Ni is effective at reducing the oxygen content of the oxygenated biomass derivatives, degrading tar [32] as well as promoting H_2 production during the pyrolysis of biomass [34]. In the supercritical water (SCW) regime, transition metals such as Ni and Pt have been reported to accelerate steam reforming, methanation, and the cleavage of C-O and C-C bonds [35]. However, precious metal catalysts such as Pt are generally used for the aqueous phase reforming (APR) of small sugar alcohols and oxygenated biomass derivatives to H_2 [36,37]. Extensive literature exists on the conversion of biomass to H_2 via pyrolysis, gasification and hydrothermal gasification, in the presence of Ni [26–31], yet they do not focus specifically on the mechanisms involved.

Recently, significant efforts have been focused on the development of catalysts from earth abundant materials (e.g., Fe and Cu). Copper has been shown to be an effective stabilizer [38] while simultaneously promoting the WGS reaction [36,39], and the reforming of small biomass-derived compounds such as methanol (in SCW) [40,41] and glycerol (for APR) [36]. Co is also reported to be effective in promoting the WGS [42] as well as decomposing tars [42–44].

While these catalysts haven been effective at converting biomass into smaller molecules, it is difficult to predict their activities in the presence of large amount of hydroxides since in-situ carbon capture via mineral carbonation could significantly shift the overall reaction equilibrium as well as generate intermediates from biomass. Thus, in this study, the pathway of H_2 production from cellulose via ATT, illustrated as Eq. (1), is investigated in the presence of a series of supported metal catalysts (i.e., Fe, Cu, Co, Pd, Pt and Ni).

$$C_6H_{10}O_5 + 6Ca(OH)_2 + H_2O \rightarrow 12H_2 + 6CaCO_3 \quad (1)$$

In addition, in-situ and ex-situ catalytic reactions (Fig. 1) are performed, in order to investigate whether solid phase or gas phase reactions dominate the ATT of cellulose. The conclusions of this study bear a significant impact on whether this technology can be scaled up, since catalyst recyclability, lifetime, and environmental concerns are significant and challenging. Finding a catalyst that retains its activity for H_2 production even when placed ex-situ of the ATT reaction would be the most optimal solution.

Materials & methods

Catalyst synthesis

Low-loading catalysts were synthesized using the incipient wetness technique whereby the metal of choice (i.e., Fe, Cu, Co, Pd, Pt and Ni) was impregnated into the support (i.e., α-Al_2O_3 and ZrO_2) via a metal salt solution. The amount and concentration of the solution needed to deposit a known quantity of metal was calculated by the water uptake capacity

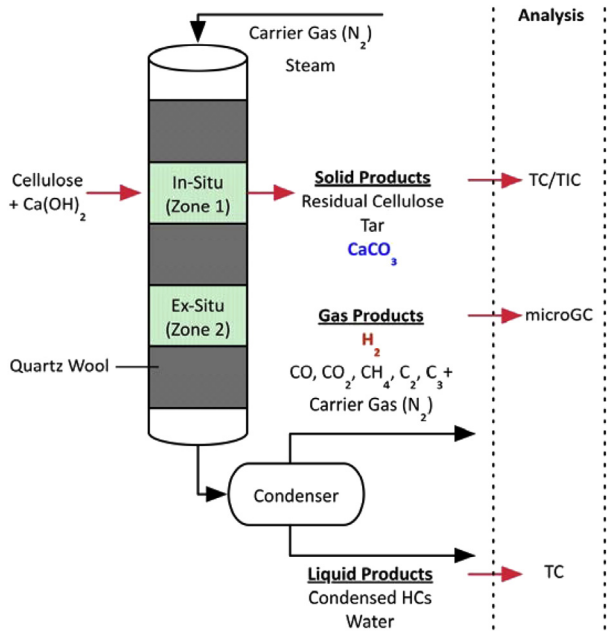

Fig. 1 – Experimental setup illustrating catalyst placement (in-situ vs. ex-situ) and sample collection points.

of the support material. High-loading catalysts on the other hand were prepared via the slurry method as described in previous work [6]. The properties of the synthesized catalyst particles are summarized in Table 1.

The metal wt% in each catalyst corresponded to four times of a theoretical monolayer coverage related to the surface area of the support and the size of the metal atom except in a few select cases (i.e., *10 wt% Ni/α-Al_2O_3*, *0.48 wt% Ni/ZrO_2* and *10 wt % Ni/ZrO_2*). Thus, different metal loadings were used for each element due to their varying atomic radii and molecular weight. A theoretical coverage of four mono-layers was chosen to keep the metal loading relatively low when compared to the 10 wt% used in previous studies [6] while simultaneously attempting to fully coat the support surface.

The impregnated supports were then dried at 363 K overnight followed by calcination in air while heating at a rate of 0.4 K/min to 563 K, followed by an isothermal treatment of 2 h. The supported catalysts were then reduced in pure H_2 at 773 K for 1 h, followed by a passivation step at 293 K. Passivation was performed by flowing 1% O_2 + 99% N_2 over the catalyst to oxidize the surface defect sites, in order to protect the metal from bulk oxidation when exposed to the ambient air. Inclusion of this passivation step resulted in increased conversion for all the catalysts, with the nickel based ZrO_2 catalyst showing higher conversion than in previously published work [6].

Table 1 – Properties of prepared supported metal catalysts.

Catalyst	BET specific surface area (m^2/g)	Average particle size (μm)
α-Al_2O_3	1.4	95.1
ZrO_2	87.6	226.8
0.48% Ni/α-Al_2O_3	1.7	66.8
10% Ni/α-Al_2O_3	0.5	177.9
0.48% Ni/ZrO_2	78.5	97.2
10% Ni/ZrO_2	71.0	139.9
0.55% Cu/α-Al_2O_3	1.7	55.5
0.42% Fe/α-Al_2O_3	1.6	56.8
0.46% Co/α-Al_2O_3	2.0	52.7
1.12% Pt/α-Al_2O_3	1.6	47.8
0.68% Pd/α-Al_2O_3	1.1	70.7

Sample preparation

Reaction samples were prepared by combining $Ca(OH)_2$ powder (Acros) with cellulose powder (Acros, micro-crystalline 50 μm particle size) at a 6:1 M ratio according to the stoichiometry given in Eq. (1). Catalyst was then added (except in baseline measurements) in order to create an overall mixture of which 20 wt% of the sample was catalyst. A small amount of water was added to the mixed powder sample in order to further promote mixing and create a sample paste. The paste was then shaped into a pellet and housed between two pieces of quartz wool inside a 1.05 cm I.D. quartz tube, which acted as the reaction vessel. Previous experiments have shown that quartz was inert during the ATT reactions [6]. The quartz tube was then placed inside the furnace, which was housed in an outer hotbox in order to keep all of the reactor lines heated.

In-situ and ex-situ catalytic reactions

Two reaction schemes were developed whereby the placement of the prepared catalyst was altered in order to elucidate the pathways of H_2 production from the ATT of cellulose (Fig. 1). Cellulose and $Ca(OH)_2$ mixtures were always placed in Zone 1, whereas the catalyst could be placed in both Zone 1 or 2. If the catalyst was placed in Zone 1 (denoted as the "in-situ" case), intimate contact between the reactants and the catalyst particles was achieved, therefore allowing solid-solid as well as gas phase catalytic reactions to take place. On the other hand, placing the catalyst in Zone 2 (denoted as the "ex-situ" case) prevented any direct solid-solid contact between the catalyst and the cellulose and $Ca(OH)_2$ mixture. Thus, any catalytic effect would arise only from the interactions between the catalyst and the gaseous compounds produced upstream via the ATT of cellulose and $Ca(OH)_2$.

Reaction conditions

Initially, N_2 flowed at a rate of 20 mL/min to purge the reactor of O_2. The purge was deemed complete once the micro-GC could not longer detect any O_2 in the exiting gas. The reaction was then initiated by heating the furnace and the outer hotbox to 373 K at a rate of 4 K/min and holding isothermally for a period of 20 min. This allowed the sample to dry prior to the reaction. After the 20-min isothermal period, liquid water was injected into the hotbox at a flow rate of 0.007 mL/min to create steam for the ATT reaction. The reactor was then heated to 773 K at a rate of 4 K/min. After the temperature ramping phase, the reactor was kept at isothermal conditions for 3 h, while collecting the gas and liquid samples. Light gases were analysed in quasi real-time, while solid and liquid samples were extracted from the quartz tube and the

condenser respectively, for analyses after cooling the entire system.

Analyses of gas and solid samples

As shown in Fig. 1, there were three sampling points for gas, liquid and solid samples. Light gases such as H_2, CO, CO_2, CH_4, C_2H_6, and C_2H_4 were quantified using an Inficon micro-GC 3000 with a sampling time of approximately 2.5 min. The sampling time was fast enough to generate kinetic curves for the formation of the light gaseous species including H_2. The light gases were also collected in a tedlar gasbag downstream of the micro-GC for the final analysis to determine the overall conversion to H_2 based on the reaction stoichiometry given in Eq. (1). All the experimental results were normalized to the moles of cellulose used in order to enable accurate comparisons.

Solid samples were collected post-reaction and analysed using a UIC Total Carbon (TC) analyser, which oxidized the samples in a pure O_2 atmosphere at 1173 K to liberate all of the carbon in the sample as CO_2. The amount of CO_2 released was then correlated to the total carbon content of the sample. Total Inorganic Carbon (TIC) analysis (acid digestion) was also used to quantify the amount of inorganic carbon ($CaCO_3$) via in-situ CO_2 capture.

Results and discussion

Low-loading metal catalysts on gas yields of cellulose pyrolysis

In order to compare the conventional pyrolysis of cellulose to the proposed ATT scheme, a series of experiments were performed using mixtures of the prepared catalysts and cellulose without any $Ca(OH)_2$. Fig. 2 illustrates that at relatively low metal loadings (≪ 10 wt%), Pt, Pd and Ni catalysts slightly increase the yield of H_2, although the overall extents of H_2 production are not significant, in comparison to non-catalytic pyrolysis. Furthermore, there is no observable trend on CO, CO_2 and CH_4 production, suggesting that for the purposes of this study, any effect of the investigated catalysts on cellulose pyrolysis is not significant.

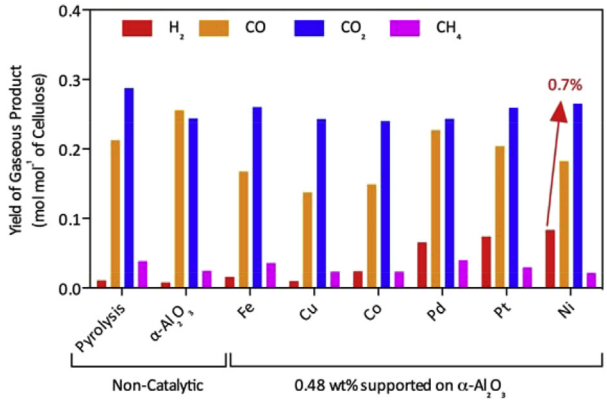

Fig. 2 – Effect of various low-loading metal catalysts supported on α-Al_2O_3 on the yields of H_2, CO, CO_2 and CH_4 during cellulose pyrolysis.

Effects of various metal catalysts on H_2 formation from Cellulose and $Ca(OH)_2$ mixture via ATT

A series of experiments was designed to compare the catalytic effects of various metals on the ATT of cellulose in terms of both gas-phase and solid-phase reactions. Here, metal catalysts were placed in in-situ and ex-situ of the ATT reaction between cellulose and $Ca(OH)_2$. As shown in Fig. 3, there are significant differences between the H_2 produced through the in-situ and ex-situ placement of the catalysts, particularly for Ni.

As a baseline measurement, the ATT of cellulose was performed in the absence of catalyst and only with the catalyst support material (i.e., ATT with α-Al_2O_3). These two cases are compared with the cellulose pyrolysis data from Fig. 2. In both cases, notable amounts of H_2 formation is observed, indicating that the presence of hydroxide (i.e., $Ca(OH)_2$) is critical to produce H_2 from cellulose. The presence of α-Al_2O_3 slightly increases the yield of H_2 from ATT of cellulose, but the difference is relatively minor.

Comparing the in-situ cases with the baseline data associated with the non-catalytic ATT of cellulose, metals such as Fe and Cu show minimal activity. The minor enhancements in the in-situ H_2 production from 4.3% to 5.0% are small in comparison to the baselines, thus Fe and Cu are eliminated from the subsequent studies.

The next set of metals, Co, Pt and Pd, show interesting effects on H_2 formation, with Pd and Pt leading to improved in-situ H_2 yields (8.6% and 8.4% respectively). On the other hand, when placed downstream of the reactants (cellulose and $Ca(OH)_2$), the H_2 yields remain similar to that of non-catalytic ATT of cellulose. These findings suggest that the mechanisms of H_2 formation in the presence of low-loading Co, Pd and Pt catalysts are dominated by solid-phase catalysis therefore indicating that the placement of catalysts plays an important role in the ATT of cellulose.

Comparing all the cases investigated, Ni is the most effective catalyst for cellulose ATT with the highest in-situ conversion to H_2: 12.0%. When the same Ni catalyst was tested in the pyrolysis reaction (Fig. 2), the conversion to H_2 was only 0.7%, therefore indicating that the presence of $Ca(OH)_2$ is necessary in order for the Ni catalyst to produce H_2.

The most interesting finding is the comparison between the in-situ and ex-situ cases for the ATT of cellulose in the presence of the Ni-based catalyst. Unlike other catalytic cases, Ni catalyst shows an enhancement in H_2 production in both reaction schemes, yet the overall conversion to H_2 is still less in the ex-situ case than the in-situ case (7.6% versus 12.0%, respectively). Ex-situ placement of the Ni-based catalyst separates the reactants (cellulose and $Ca(OH)_2$) from the catalyst, therefore the difference in conversion between the non-catalytic case and the ex-situ Ni case shown in Fig. 3 (a) can be attributed to the conversion of gaseous intermediates/by-products generated via the non-catalytic ATT reaction. This suggests that although the intermediates formed during cellulose ATT are not fully identified at this time, the Ni catalyst promotes both solid phase and gas phase reactions associated

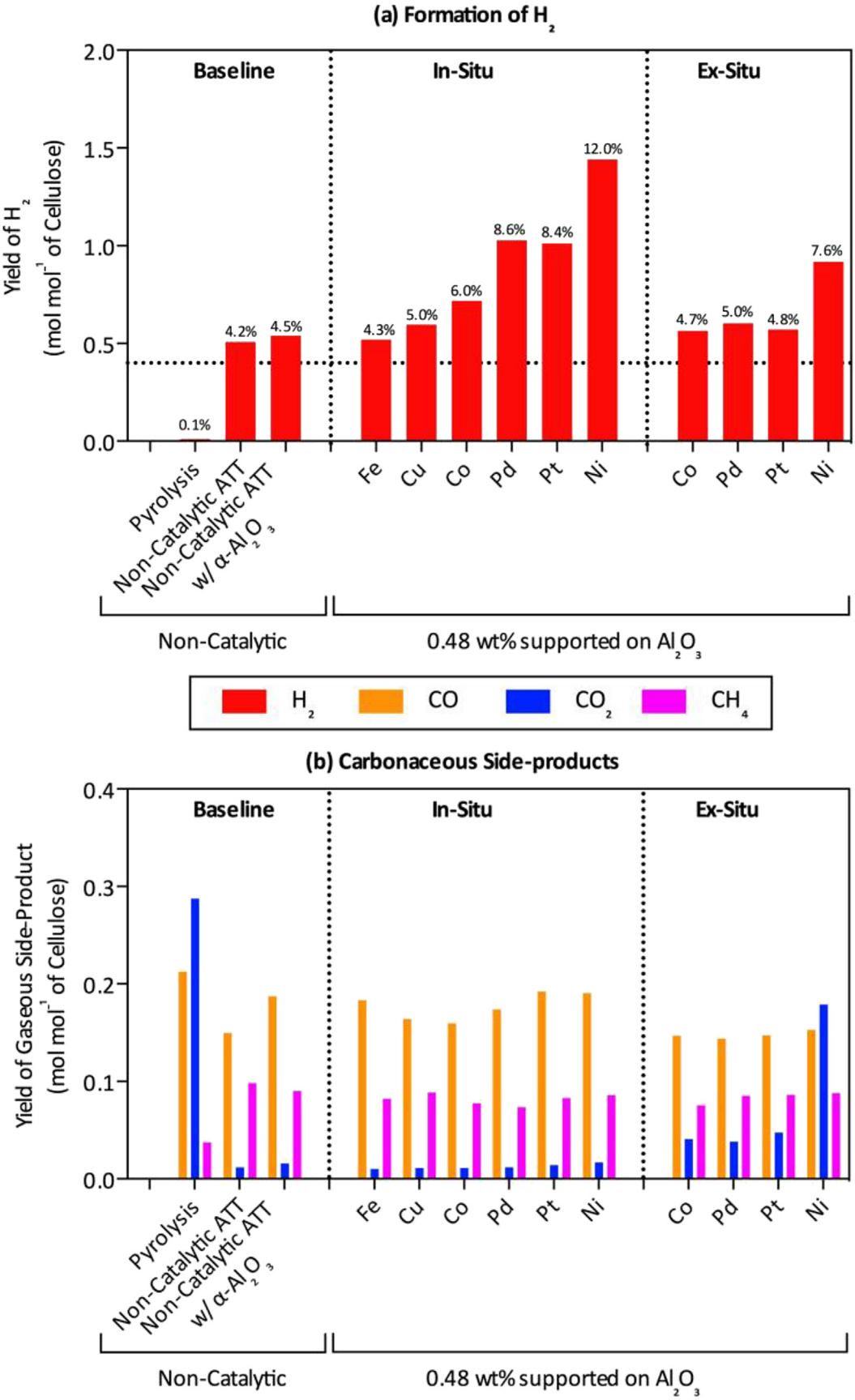

Fig. 3 – Effects of various low-loading metal catalysts supported on α-Al_2O_3 on the yields of H_2, CO, CO_2 and CH_4 from the reaction of cellulose + $Ca(OH)_2$ while altering the location of catalyst placement.

with the reaction between cellulose and $Ca(OH)_2$. Therefore, amongst the tested metals, the Ni-based catalyst is the best candidate for the ATT of biomass and allows for greater flexibility when optimizing future reactor designs.

The novelty of the ATT of biomass is its ability to produce H_2 with supressed CO_2 formation by locking the carbon into a stable carbonate form. Hence, in order to further investigate the reaction pathways of cellulose ATT, it is important to analyse other gaseous products (e.g., CO, CO_2, and CH_4). As shown in Fig. 3 (b), no general trends for CO, CO_2 and CH_4 formations seem to be apparent for all ATT cases, particularly for in-situ cases. However, when the catalysts (Co, Pd, Pt and Ni) were placed downstream of the ATT reaction (ex-situ case), the amount of CO_2 in the gaseous product notably increases while the in-situ cases show no noticeable increase in the amount of CO_2 when comparing to the non-catalytic ATT level. This suggests that CO_2 and H_2 formation are related and that $Ca(OH)_2$ is acting as an in-situ CO_2 sorbent as well as a reactant that promotes H_2 production. Specifically, in-situ CO_2 capture by $Ca(OH)_2$ is demonstrated by the low CO_2 concentration observed in the in-situ reaction with Ni. Even at the highest H_2 formation, the level of CO_2 is maintained similar to that of the non-catalytic ATT reaction illustrating a promising BECCS potential.

This dual effect of $Ca(OH)_2$ is expected as it has been shown that the addition of either CaO or $Ca(OH)_2$ in gasification reactions can promote the yield of H_2 from biomass. This is due to the cracking of larger compounds, however the precise mechanism is not detailed [9–12]. Since Ni shows a greater effect over other metals studied and is less expensive than metals such as Pt and Pd (according to the latest S&P indices), subsequent experiments focused on understanding the ATT reaction pathways of H_2 production over various Ni-based catalysts.

Effect of Ni loading on the ATT of cellulose

To further investigate the complex reaction pathways of the ATT of cellulose in both gas and solid phases, catalysts with two different Ni-loadings (0.48 and 10 wt%) were prepared and their gaseous formation behaviours was studied. Figs. 4 and 5 show the formation rates of the main gases of interest (i.e., H_2, CO, CO_2 and CH_4) as a function of temperature when cellulose was reacted with $Ca(OH)_2$ with and without the Ni/α-Al_2O_3 catalyst.

The first interesting observation is that the placement of the catalyst (i.e., in-situ or ex-situ) does not cause a shift in the peak formation temperatures for H_2 occurring at ~640 K and ~770 K (Fig. 4). This suggests that the primary pathways of H_2 production in the presence of Ni/α-Al_2O_3 catalyst does not change by placing the catalyst in contact with the biomass/hydroxide solid mixture or downstream only for subsequent gas reforming. The first H_2 generation curves are similar for all three cases (i.e., non-catalytic ATT, in-situ catalytic ATT and ex-situ catalytic ATT) illustrating that Ni-based catalyst is not effective at enhancing the first reaction pathway of H_2 formation via cellulose ATT. The majority of the enhancement in H_2 formation occurs at elevated temperatures (>700 K). This is expected since Ni is known to enhance the cracking of higher molecular weight hydrocarbons and oxygenates at elevated temperatures in order to produce H_2 [45–48]. The difference between formation curves of the in-situ and ex-situ cases shown in Fig. 4 (a), suggests that Ni-based catalyst is involved in both the breakdown of cellulose, and the conversion of the gaseous intermediates to H_2. Based on Fig. 4 (b) and (d), H_2 production mechanisms such as the water-gas shift (WGS) reaction and steam methane reforming (SMR) may be ruled out since CO and CH_4 concentrations in the gaseous product stream do not change significantly between all three cases. The major difference is the increased CO_2 formation at higher reaction temperatures when the Ni catalyst is placed ex-situ. In other words, the formation of H_2 over the Ni catalyst via gas reforming results in CO_2 as by-product, which cannot be captured since it generated downstream of $Ca(OH)_2$.

The ATT of cellulose in the presence of 0.48 wt% Ni/α-Al_2O_3 catalyst shown in Fig. 4 has provided important insights into how this complex and yet unique biomass conversion to H_2 occurs. However, the overall cellulose conversion to H_2 is limited to only 12.0%. Consequently, a higher loading Ni/α-Al_2O_3 catalyst (10 wt%) was tested in order to determine whether the reaction was limited by low metal content.

As shown in Fig. 5, the formation of H_2 increases, with an overall cellulose conversion to H_2 of 16.6% and 13.3% for in-situ and ex-situ cases, respectively. When comparing the 10 wt% Ni/α-Al_2O_3 (Fig. 5) to the 0.48 wt% Ni/α-Al_2O_3 (Fig. 4) catalyst, the peak H_2 formation temperatures and trends are quite similar; H_2 is produced in conjunction with CO_2, and there is little evidence of the WGS and SMR reactions. Furthermore, although there is a slight enhancement observed in the first peak at 640 K in the case of 10 wt% Ni/α-Al_2O_3, the majority of the H_2 is still produced at elevated temperatures: >700 K.

The H_2 formation curves alone are not enough to explain how the ATT of cellulose produces H_2. However, the strong correlation between H_2 and CO_2 concentrations in the gaseous product stream (illustrated in Fig. 5 (a) and (c) as well as Fig. 4) suggests that H_2 formation may not be dominated by solid-solid catalysis but rather by the gaseous reforming of hydrocarbons. Thus, the placement of the Ni-based catalyst is important for the enhanced H_2 production via ATT, while the proximity of hydroxide to the catalyst determines the extent of carbon capture during the biomass conversion.

Effect of surface area of catalyst support on the ATT of cellulose

Originally, it was hypothesized that the ATT of biomass was likely dominated by solid-solid interactions between the cellulose, $Ca(OH)_2$ and 10% Ni/ZrO_2 particles. Under this assumption, mass transfer limitations are significant and a high surface area catalyst would be largely ineffective at promoting reactions that are dependent on the interfacial area between the particles. However, the findings from the in-situ and ex-situ studies highlighted the importance of the gas phase catalysis for H_2 production; therefore, a higher surface area support (i.e., ZrO_2) was selected to further investigate the ATT of cellulose.

Four sets of Ni-based catalysts were prepared using low surface area α-Al_2O_3 (1.4 m^2/g) and high surface area ZrO_2 (87.6 m^2/g) for ZrO_2) with different Ni loadings (i.e., 0.48 wt%

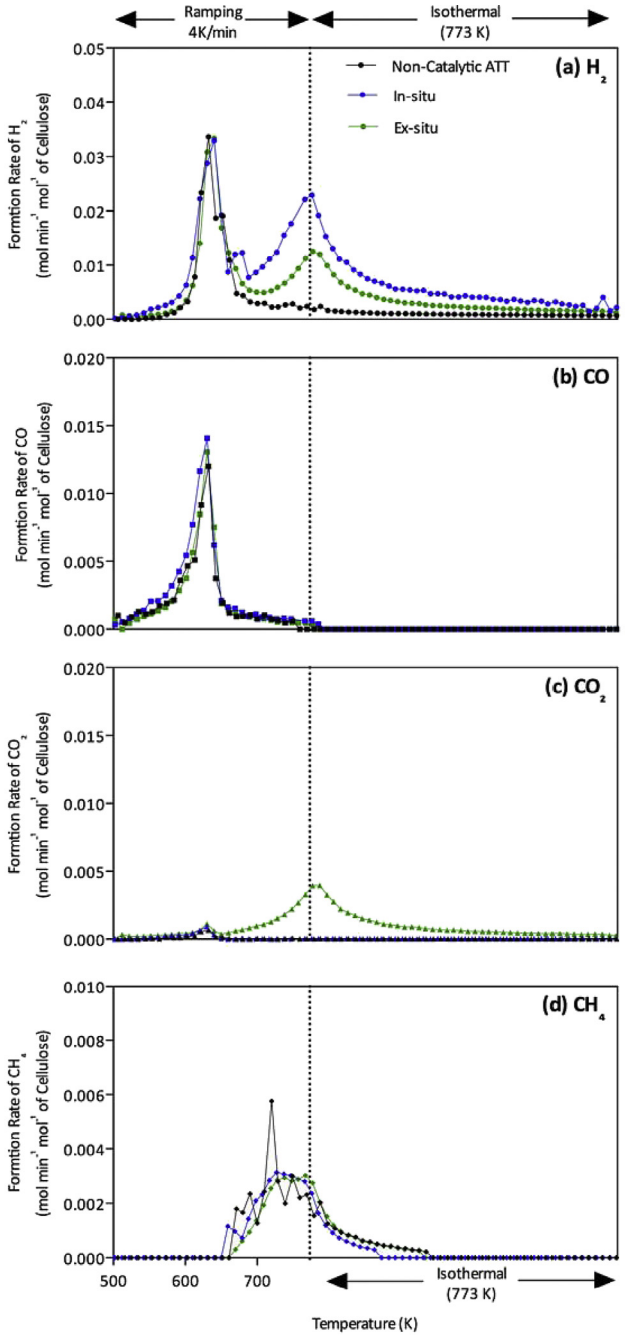

Fig. 4 – Formation Rates of H_2, CO, CO_2, and CH_4 from ATT of cellulose in the presence of 0.48 wt% Ni/α-Al_2O_3 placed to promote gas and/or solid phase reactions.

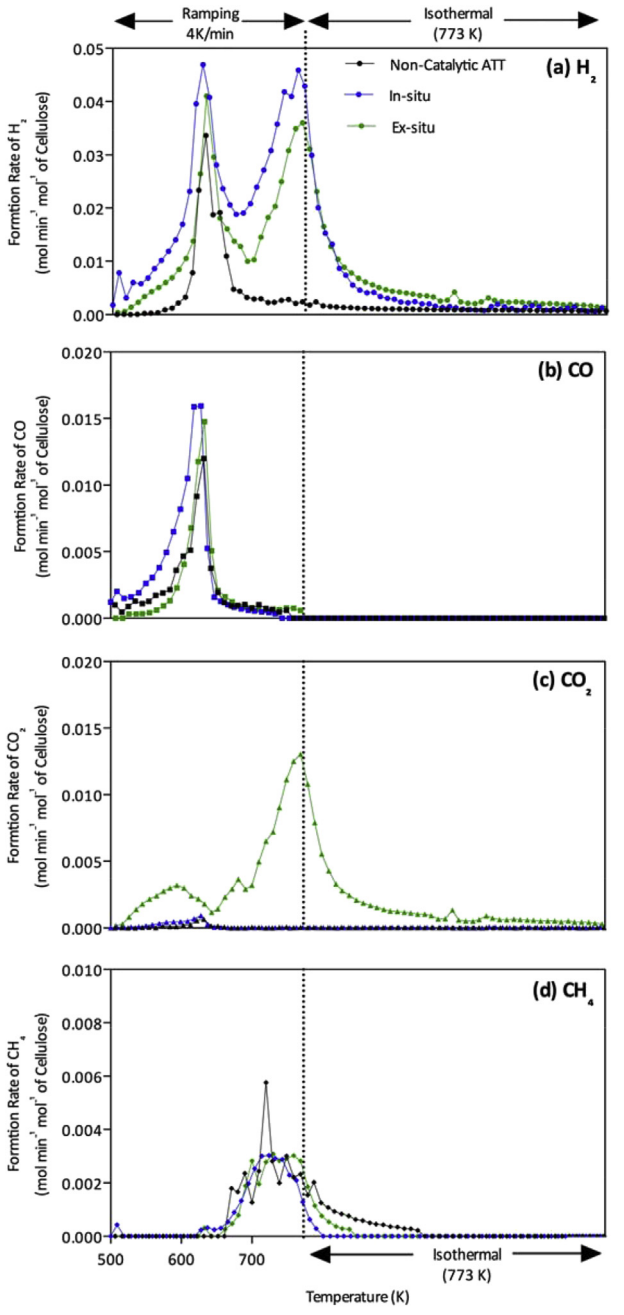

Fig. 5 – Formation Rates of H_2, CO, CO_2, and CH_4 from ATT of cellulose in the presence of Ni/α-Al_2O_3 with increased Ni-loading (10 wt%).

and 10 wt%). As shown in Fig. 6, ZrO_2-supported catalysts show greater activities in promoting H_2 production compared to those prepared with α-Al_2O_3. At low loading, impregnating 0.48 wt% Ni on ZrO_2 instead of α-Al_2O_3 shows an increase in the cellulose conversion to H_2 from 12.0% to 17.2% and from 7.6% to 8.8% for the in-situ and ex-situ cases, respectively.

The difference between the supports is more evident at high Ni loadings. 10 wt% Ni/α-Al_2O_3 results in an in-situ conversion of 16.6%, however, the same metal loading on ZrO_2 results in a conversion of 49.0%. Similar to the results shown in Fig. 3, when the catalyst is placed downstream of the ATT reaction, a higher H_2 formation is associated with increased CO_2 concentration in the outlet gas stream (Fig. 9) due to the absence of CO_2 absorbing $Ca(OH)_2$. The formation trends of other gases (CO and CH_4) are not significantly altered as different catalyst supports are employed.

Fig. 6 illustrates that both the type of catalyst support and the amount of Ni loading are important for enhanced H_2 formation. To further explain the difference between the

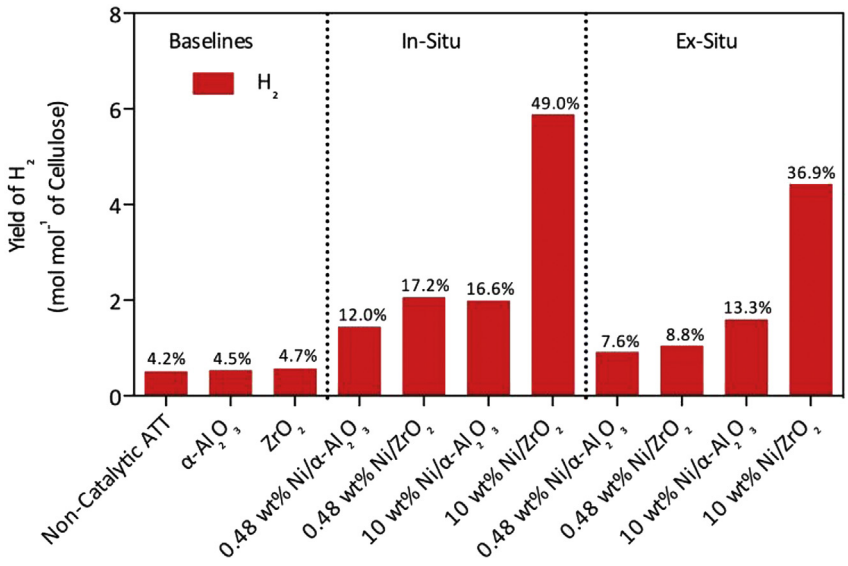

Fig. 6 – H_2, yields from the reaction of cellulose + $Ca(OH)_2$ in the presence of Ni-based catalyst supported on two separate supports with different surface areas: α-Al_2O_3 and ZrO_2.

activities of Ni on ZrO_2 and α-Al_2O_3, CO chemisorption and BET analyses were performed.

The data in Table 2 shows that an increase in the amount of exposed metal does not necessarily correlate linearly with an increase in the conversion to H_2. In both the case of Ni supported on α-Al_2O_3 and ZrO_2, despite an increase in the amount of exposed metal by factors of 9.9 and 43.1 respectively, the conversion to H_2 does not increase by these factors. This suggests that both α-Al_2O_3 and ZrO_2-based Ni catalysts are not kinetically limited but rather may be limited by mass transfer limitations through the catalyst pores. The pore size distributions of the catalysts are shown in Fig. 7 and indicate that ZrO_2 is far more mesoporous than α-Al_2O_3, consequently the diffusion of gases through the pores in ZrO_2 should be quicker than in α-Al_2O_3, leading to a higher catalytic conversion of gaseous intermediates to H_2.

From Table 2 it is evident that a higher loading corresponds to a higher CO chemisorption value, however, this does not imply that 10 wt% Ni loading is optimal. The metal loadings used in this study were selected to compare the activity of different metals at low (0.48 wt%) and relatively high (10 wt%) metal loadings in order to establish a general trend in activity and selectivity. Determining the optimal coverage of metal on the support extends beyond determining the theoretical monolayer coverage; the synthesis procedure plays an important role in the dispersion of metal in the final catalyst, which will have an impact on catalytic performance. More detailed studies are necessary to identify the optimal loading for each metal through optimization of the synthesis technique.

Table 2 – Amount of Exposed Metal in the Ni-based catalysts prepared using α-Al_2O_3 and high surface area ZrO_2 and their performances in H_2 production via ATT of cellulose.

Catalyst	In-situ conversion to H_2 (%)	Exposed metal (CO chemisorption) (μmol/g)
0.48 wt% Ni/α-Al_2O_3	12.0	1.45
10 wt% Ni/α-Al_2O_3	16.6	14.34
0.48 wt% Ni/ZrO_2	17.2	1.56
10 wt% Ni/ZrO_2	49.0	67.31

Proposed reaction pathways of H_2 formation via the ATT of cellulose

The findings from the in-situ and ex-situ experiments can now be used to elucidate the potential H_2 production pathways during the ATT of cellulose. H_2 production in the in-situ cases are attributed to both solid phase and gas phase reactions but can be broken down into its separate components by using ex-situ and baseline data. Fig. 8 shows how H_2 is produced according to its reaction phase. At low Ni loadings the relative amount of H_2 produced due to solid-solid catalysis in comparison to the total is larger since the gas phase reactions are limited due to a lower quantity of exposed Ni metal available (as listed in Table 2). However, as the Ni loading is

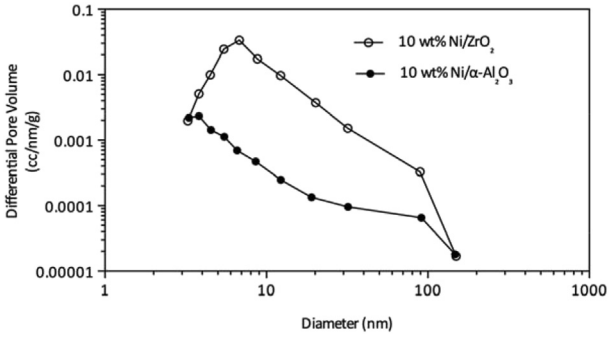

Fig. 7 – Differential pore volume distribution of the fresh 10% Ni-based catalysts supported on ZrO_2 and α-Al_2O_3.

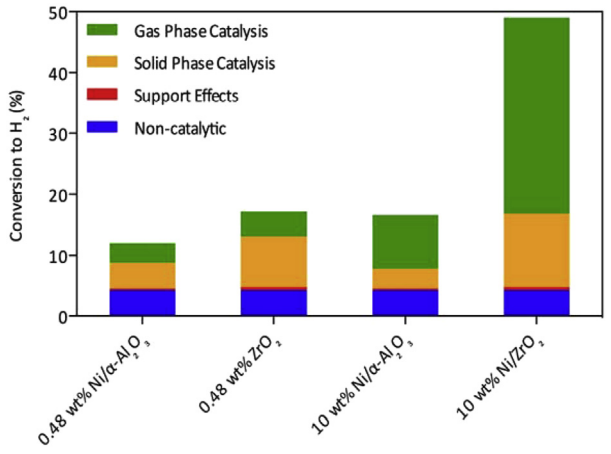

Fig. 8 – Comparison of Ni-based catalysts prepared with different Ni-loadings and support materials in terms of their mechanisms of H_2 production from cellulose and $Ca(OH)_2$ via ATT.

increased, gas phase H_2 reforming becomes far more dominant as shown in the case of 10 wt% Ni/ZrO_2. In both the case of ZrO_2 and α-Al_2O_3, despite an approximate 20-fold increase in Ni content (from 0.48 wt% to 10 wt%) and an increase in exposed metal, the H_2 produced via solid catalysis does not change in tandem. This indicates that the primary mechanism of H_2 production is through gaseous reforming when Ni loading is sufficiently high. However, considering the greater overall H_2 production observed in in-situ cases compared to ex-situ cases (shown in Fig. 3), it should also be noted that the solid phase catalysis still plays an important role in producing gaseous intermediates that are being reformed to H_2.

Bio-Energy with Carbon Capture and Storage (BECCS) potential of ATT of cellulose

In order to evaluate the BECCS potential of the novel ATT reaction of biomass, it is important to investigate the distribution of carbon throughout the product streams (both solid and gaseous streams) in addition to the H_2 formation behaviour. Fig. 9 shows the fate of carbon in the solid residues and

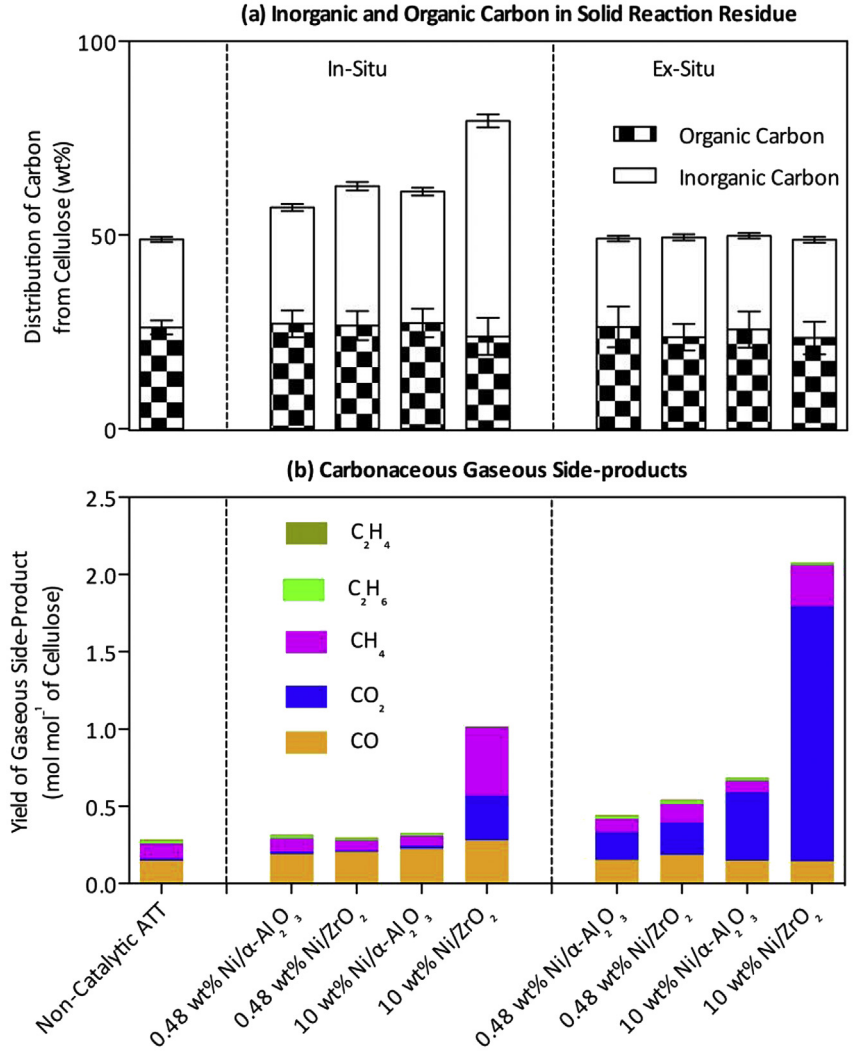

Fig. 9 – Comparison of Ni-based catalysts prepared with different Ni-loadings and support materials in terms of carbon distribution in products and reaction residues.

gaseous by-products from cellulose in the presence of various catalysts.

Fig. 9 (a) shows that the solid residue is found to contain both inorganic and organic carbon, with the in-situ reactions having similar levels of organic carbon to the baseline, thus indicating that the catalysts may only have a minor effect on the extent of cellulose degradation. Conversely, inorganic carbon is much higher than the baseline in the case of the most active catalyst; 10 wt% Ni/ZrO_2. This increase is caused by the carbonation of CO_2 formed via the reforming of hydrocarbons to H_2 and CO_2 over the Ni-catalyst. This is corroborated by Fig. 9 (b) that shows significant suppression of CO_2 in-situ, except in the case of 10 wt% Ni/ZrO_2, where some CO_2 is produced, which may be attributed to the kinetics of carbonation being slower than the kinetics of CO_2 formation via reforming.

The ex-situ case shows that inorganic and organic carbon amounts are similar to the non-catalytic ATT case, which is expected since the catalysts in each case are all placed downstream of the cellulose and $Ca(OH)_2$. Consequently, the yield CO_2 is much higher than non-catalytic case as shown in Fig. 9 (b). The reforming reactions occur away from the $Ca(OH)_2$ and therefore there is no CO_2 capture material. These results indicate that H_2 formation occurs primarily in the gas-phase and all of the tested catalysts have a much smaller effect in term of solid-solid catalysis. However due to this pathway of H_2 production, significant levels of CO_2 may only be captured, when the catalyst is placed in-situ.

Conclusions

This study has shown that the catalytic activities of the various metals tested for H_2 production follow the trend: Ni > Pt, Pd > Co > Fe, Cu. The choice of the support is critical in achieving a high conversion as illustrated by ZrO_2 supported Ni catalysts, which show much greater catalytic activity than their α-Al_2O_3 counterparts. This is due to their larger surface area, increased metal dispersion and larger fraction of mesopores. It was found that H_2 production is controlled through the reforming of gaseous intermediates over the Ni catalyst, and although solid contact between the catalyst and the reactants does yield slight improvements over pure gas phase catalysis, it does not scale with the number of exposed Ni sites. However, for suppressed CO_2 formation, the catalyst must be intimately mixed with the reactants in order to allow for the formation of $CaCO_3$ from the carbonation of the produced CO_2 with $Ca(OH)_2$. Alternate mechanisms for H_2 production, such as the WGS and CH_4 reforming were ruled out due to relatively low and constant CO and CH_4 formation curves. Overall, the 10% Ni/ZrO_2 catalyst was the most effective at promoting H_2 yield, with a maximum conversion of 49.0%. Although results from the current study revealed that Ni showed better performance than both precious metals (Pd and Pt) and other non-precious metals (Co, Cu and Fe), more detailed studies are necessary to understand the origin of the unique activity through mechanistic studies involving the likely oxygenated intermediates that are present.

Acknowledgements

The authors acknowledge NSF CBET 1336567 for financially funding this work. We also would like to thank Congwei Fei, Menjia Wang, Foyinsola Bolade, and Charlie Wu for their help with this project.

REFERENCES

[1] EIA. EIA projects world energy consumption will increase 56% by 2040. US Energy Information Administration; 2013. http://www.eia.gov/todayinenergy/detail.cfm?id=12251. [Accessed 3 November 2014].
[2] Jenkins BM, Baxter LL, Miles Jr TR, Miles TR. Combustion properties of biomass. Fuel Process Technol 1998;54:17–46.
[3] Pachauri RK, Meyer LA. IPCC, 2014: climate change 2014: synthesis report. Geneva, Switzerland. 2014.
[4] Ferguson TE, Park Y, Petit C, Park A-HA. Novel approach to hydrogen production with suppressed CO_x generation from a model biomass feedstock. Energy Fuels 2012;26:4486–96. http://dx.doi.org/10.1021/ef300653b.
[5] Ishida M, Otsuka K, Takenaka S, Yamanaka I. One-step production of CO- and CO_2-free hydrogen from biomass. J Chem Technol Biotechnol 2005;80:281–4. http://dx.doi.org/10.1002/jctb.1188.
[6] Stonor MR, Ferguson TE, Chen JG, Park A-HA. Biomass conversion to H_2 with substantially suppressed CO_2 formation in the presence of Group I & Group II hydroxides and a Ni/ZrO_2 catalyst. Energy Environ Sci 2015;8:1702–6. http://dx.doi.org/10.1039/C4EE04103H.
[7] Florin NH, Harris AT. Hydrogen production from biomass coupled with carbon dioxide capture: the implications of thermodynamic equilibrium. Int J Hydrogen Energy 2007;32:4119–34.
[8] Florin NH, Harris AT. Enhanced hydrogen production from biomass with in situ carbon dioxide capture using calcium oxide sorbents. Chem Eng Sci 2008;63:287–316.
[9] Guoxin H, Hao H. Hydrogen rich fuel gas production by gasification of wet biomass using a CO_2 sorbent. Biomass Bioenergy 2009;33:899–906.
[10] Mahishi MR, Goswami DY. An experimental study of hydrogen production by gasification of biomass in the presence of a sorbent. Int J Hydrogen Energy 2007;32:2803–8.
[11] Acharya B, Dutta A, Basu P. An investigation into steam gasification of biomass for hydrogen enriched gas production in presence of CaO. Int J Hydrogen Energy 2010;35:1582–9.
[12] Hanaoka T, Yoshida T, Fujimoto S, Kamei K, Harada M, Suzuki Y, et al. Hydrogen production from woody biomass by steam gasification using a sorbent. Biomass Bioenergy 2005;28:63–8.
[13] Fricker KJ, Park A-HA. Effect of H_2O on $Mg(OH)_2$ carbonation pathways for combined CO_2 capture and storage. Chem Eng Sci 2013;100:332–41.
[14] Shimada N, Kawamoto H, Saka S. Different action of alkali/alkaline earth metal chlorides on cellulose pyrolysis. J Anal Appl Pyrolysis 2008;81:80–7.
[15] Muangrat R, Onwudili JA, Williams PT. Influence of alkali catalysts on the production of hydrogen-rich gas from the hydrothermal gasification of food processing waste. Appl Catal B Environ 2010;100:440–9.

[16] Waldner MH, Vogel F. Renewable production of methane from woody biomass by catalytic hydrothermal gasification. Ind Eng Chem Res 2005;44:4543–51. http://dx.doi.org/10.1021/ie050161h.
[17] Onwudili JA, Williams PT. Hydrothermal reactions of sodium formate and sodium acetate as model intermediate products of the sodium hydroxide-promoted hydrothermal gasification of biomass. Green Chem 2010;12:2214. http://dx.doi.org/10.1039/c0gc00547a.
[18] Raveendran K, Ganesh A, Khilar KC. Influence of mineral matter on biomass pyrolysis characteristics. Fuel 1995;74:1812–22.
[19] Kumar S, Drozd V, Saxena S. Catalytic studies of sodium hydroxide and carbon monoxide reaction. Catalysts 2012;2:532–43.
[20] Knill CJ, Kennedy JF. Degradation of cellulose under alkaline conditions. Carbohydr Polym 2003;51:281–300.
[21] Davidson GF. The dissolution of chemically modified cottong cellulose in alkaline solutions. part I – in solutions of sodium hydroxide, particularly at temepratures below the normal. J Text Inst Trans 1934;25:T174–96. http://dx.doi.org/10.1080/19447023408661621.
[22] Ziderman I. Endwise depolymerisation of cellulose in the presence of alkaline earth hydroxides. Cellul Chem Technol 1980;14:703–11.
[23] Finch CA. In: Nevell TP, Zeronian SH, editors. Cellulose chemistry and its applications. Chichester: Ellis Horwood; 1985. p. 552. http://dx.doi.org/10.1002/pi.4980170313. price £55.00. ISBN 0-85312-463-9. Brit Poly J 1985;17:321–1.
[24] Machell G, Richards GN. Mechanism of saccharinic acid formation. Part I. Competing reactions in the alkaline degradation of 4-O-methyl-D-glucose, maltose, amylose, and cellulose. J Chem Soc 1960:1924–31. http://dx.doi.org/10.1039/jr9600001924.
[25] Machell G, Richards GN. Mechanism of saccharinic acid formation. Part II. The aB-dicarbonyl intermediate in formation of D-glucoisosaccharinic acid. J Chem Soc 1960:1932–8. http://dx.doi.org/10.1039/jr9600001932.
[26] Gong M, Zhu W, Zhang HW, Ma Q, Su Y, Fan YJ. Influence of NaOH and Ni catalysts on hydrogen production from the supercritical water gasification of dewatered sewage sludge. Int J Hydrogen Energy 2014;39:19947–54.
[27] Wu C, Wang Z, Dupont V, Huang J, Williams PT. Nickel-catalysed pyrolysis/gasification of biomass components. J Anal Appl Pyrolysis 2013;99:143–8. http://dx.doi.org/10.1016/j.jaap.2012.10.010.
[28] Pei A, Zhang L, Jiang B, Guo L, Zhang X, Lv Y, et al. Hydrogen production by biomass gasification in supercritical or subcritical water with Raney-Ni and other catalysts. Front Energy Power Eng China 2009;3:456–64. http://dx.doi.org/10.1007/s11708-009-0069-y.
[29] Matras J, Niewiadomski M, Ruppert A, Grams J. Activity of Ni catalysts for hydrogen production via biomass pyrolysis. Kinet Catal 2012;53:565–9. http://dx.doi.org/10.1134/S0023158412050096.
[30] Minowa T, Zhen F, Ogi T. Cellulose decomposition in hot-compressed water with alkali or nickel catalyst. J Supercrit Fluids 1998;13:253–9.
[31] Ishida M, Takenaka S, Yamanaka I, Otsuka K. Production of CO_x-free hydrogen from biomass and NaOH mixture: effect of catalysts. Energy Fuels 2006;20:748–53. http://dx.doi.org/10.1021/ef050282u.
[32] Buchireddy PR, Bricka RM, Rodriguez J, Holmes W. Biomass gasification: catalytic removal of tars over zeolites and nickel supported zeolites. Energy Fuels 2010;24:2707–15. http://dx.doi.org/10.1021/ef901529d.
[33] Inaba M, Murata K, Saito M, Takahara I. Hydrogen production by gasification of cellulose over Ni catalysts supported on zeolites. Energy Fuels 2006;20:432–8. http://dx.doi.org/10.1021/ef050283m.
[34] Iliopoulou EF, Stefanidis SD, Kalogiannis KG, Delimitis A, Lappas AA, Triantafyllidis K S. Catalytic upgrading of biomass pyrolysis vapors using transition metal-modified ZSM-5 zeolite. Appl Catal B Environ 2012;127:281–90. http://dx.doi.org/10.1016/j.apcatb.2012.08.030.
[35] Guo Y, Wang SZ, Xu DH, Gong YM, Ma HH, Tang XY. Review of catalytic supercritical water gasification for hydrogen production from biomass. Renew Sustain Energy Rev 2010;14:334–43.
[36] Chheda JN, Huber GW, Dumesic JA. Liquid-phase catalytic processing of biomass-derived oxygenated hydrocarbons to fuels and chemicals. Angew Chem Int Ed 2007;46:7164–83. http://dx.doi.org/10.1002/anie.200604274.
[37] Cortright RD, Davda RR, Dumesic JA. Hydrogen from catalytic reforming of biomass-derived hydrocarbons in liquid water. Nature 2002;418:964–7. http://dx.doi.org/10.1038/nature01009.
[38] Elliott DC, Hart TR, Neuenschwander GG. Chemical processing in high-pressure aqueous environments. 8. Improved catalysts for hydrothermal gasification. Ind Eng Chem Res 2006;45:3776–81. http://dx.doi.org/10.1021/ie060031o.
[39] Gokhale AA, Dumesic JA, Mavrikakis M. On the mechanism of low-temperature water gas shift reaction on copper. J Am Chem Soc 2008;130:1402–14. http://dx.doi.org/10.1021/ja0768237.
[40] Gadhe JB, Gupta RB. Hydrogen production by methanol reforming in supercritical water: catalysis by in-situ-generated copper nanoparticles. Int J Hydrogen Energy 2007;32:2374–81.
[41] Saxena RC, Seal D, Kumar S, Goyal HB. Thermo-chemical routes for hydrogen rich gas from biomass: a review. Renew Sustain Energy Rev 2008;12:1909–27.
[42] Zhao M, Florin NH, Harris AT. Mesoporous supported cobalt catalysts for enhanced hydrogen production during cellulose decomposition. Appl Catal B Environ 2010;97:142–50.
[43] Furusawa T, Tsutsumi A. Development of cobalt catalysts for the steam reforming of naphthalene as a model compound of tar derived from biomass gasification. Appl Catal General 2005;278:195–205.
[44] Wang L, Li D, Koike M, Watanabe H, Xu Y, Nakagawa Y, et al. Catalytic performance and characterization of Ni–Co catalysts for the steam reforming of biomass tar to synthesis gas. Fuel 2013;112:654–61.
[45] Shen Y, Areeprasert C, Prabowo B, Takahashi F, Yoshikawa K. Metal nickel nanoparticles in situ generated in rice husk char for catalytic reformation of tar and syngas from biomass pyrolytic gasification. RSC Adv 2014;4:40651–64. http://dx.doi.org/10.1039/C4RA07760A.
[46] Li S, Gong J. Strategies for improving the performance and stability of Ni-based catalysts for reforming reactions. Chem Soc Rev 2014;43:7245–56. http://dx.doi.org/10.1039/C4CS00223G.
[47] Production of hydrogen from steam reforming of glycerol using nickel catalysts supported on Al_2O_3, CeO_2 and ZrO_2. Catal Sustain Energy 2013;1:60–70. http://dx.doi.org/10.2478/cse-2013-0001.
[48] Gupta DV, Kranich WL, Weiss AH. Catalytic hydrogenation and hydrocracking of oxygenated compounds to liquid and gaseous fuels. Ind Eng Chem Proc Des Dev 1976;15:256–60. http://dx.doi.org/10.1021/i260058a008.